CARBON 48 (2010) 2773–2781

available at www.sciencedirect.com

ScienceDirect

journal homepage: www.elsevier.com/locate/carbon

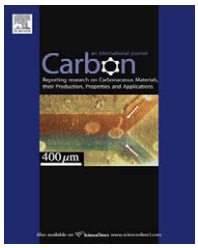

Spectroscopic and electrochemical study of hybrids containing conductive polymers and carbon nanotubes

Shoshana Ben-Valid [a], *Bea Botka* [b], *Katalin Kamarás* [b], *Aiping Zeng* [a], *Shlomo Yitzchaik* [a,*]

[a] *Institute of Chemistry and the Nanoscience and Nanotechnology Center, The Hebrew University of Jerusalem, Jerusalem 91904, Israel*
[b] *Research Institute for Solid State Physics and Optics, Hungarian Academy of Sciences, P.O. Box 49, H-1525 Budapest, Hungary*

ARTICLE INFO

Article history:
Received 25 November 2009
Accepted 3 April 2010
Available online 9 April 2010

ABSTRACT

We report the preparation and characterization of hybrid materials from conducting polymers and single walled carbon nanotubes. Electrochemical polymerization yields nanotubes wrapped by conducting polymers – polyaniline, polycarbazole and melanin (i.e., polydopamine). The materials were characterized by ultraviolet–visible–near infrared, infrared, Raman and impedance spectroscopy. We found that wrapping the nanotubes with polymers can decrease the impedance of such composite electrode and increase the rate of electron transfer from the electrolyte to the electrode. From the attenuation of in-plane vibrations in the infrared spectra and the bathochromically shifted polaron band, we infer that the strongest interaction occurs between polyaniline and the nanotube surface.

1. Introduction

Carbon nanotubes (CNTs) are widely used as additives to various other particular materials to construct new structures with tailor-made properties. In particular, the good ionic and electrical conductivity, large pseudo-capacitance and redox charge storage mechanism of conducting polymers combined with the ultra-high mechanical strength, good electrical properties, high surface area and high aspect ratio of CNTs lead to composites which are promising as electrode material in supercapacitor devices [1–3]. Such composites are also used as optical and solid state gas sensors [4] or biosensors [5], deposited on various transparent and flexible surface shapes.

There are many conductive polymers conjugated to CNTs whose properties have been studied in detail, such as polyaniline (PANI) [6], polypyrrole [7], polycarbazole (PCz) [8], poly(3,4-ethylenedioxythiophene) (PEDOT) [9], and poly-(3-(2-hydroxyethyl)-2,5-thienylene) (PHET) [10]. In this contribution we study in detail the structural and electronic interactions of CNTs with three conducting polymers: PANI, melanin and PCz. PANI is one of the most important conducting polymers, because of its relatively facile processability, electrical conductivity, reversibly controllable by proton doping and redox state, and environmental stability. Melanin [11–13] which is an attractive natural conductive polymer that can improve dramatically the biocompatibility of CNTs because it found in plants, animals and humans as a skin and hair pigment, as well as in pigment-bearing neurons within areas of the brain stem. Finally, PCz which has good thermal stability, combined with photoconductivity and its conducting form can be easily obtained by electrochemical polymerization [14–16]. Polycarbazole and its derivatives have been widely synthesized and used for a variety of applications such as sensors, light-emitting diodes and photovoltaic devices [17–20].

By conjugating CNT with the above conducting polymers we expect to improve the electronic capacitance and biocompatibility of nanotubes and the hybrid can be exploited for the design of new systems for neuronal growth and repair [21,22]. The idea of reconnecting brain signal pathways after neuronal injury is not new. However, the main problem in sensing neural activity is the poor adhesion of neurons to the device and the solution-derived shunting noise [23]. Recent advances in nanotechnology renewed the development of neural biomaterials, and investigations have started to address the

* *Corresponding author:* Fax: +972 2 658 5319.
E-mail address: sy@cc.huji.ac.il (S. Yitzchaik).
0008-6223/$ - see front matter
doi:10.1016/j.carbon.2010.04.005

issue of CNT substrates effects on neural growth [24–27]. CNT appear well suited for this design, also due to their diameters, which are very close to those of neural dendrites and resembles extracellular components. Studies on chemically modified multi-walled carbon nanotubes (MWCNT) have already suggested the potential for these materials to guide neurite outgrowth *in vitro*, by influencing neuronal extra cellular/molecular interactions [28]. However, it is not clear whether CNT could directly improve the rewiring of disconnected neuronal networks, due to their intrinsic structure and overall morphology. Moreover, the role of functionalization (i.e., the covalent attachment of functional groups or the polymer coating) of CNT on the neuron activity is still not well defined.

Recently, we have shown a novel route for the assembly of 2D-conducting polymers on template layer containing solid supports via chemical and enzymatic routes [29]. Studies of neuron outgrowth on such nanometric layers containing surfaces showed that 2D-PANI creates an intimate interface for neurons outgrowth manifested in lamellipodium formation [30]. The combinations of positively charged polymer (i.e., containing quaternary amines) and rough interface led to very strong cell adhesion to planar as well as patterned substrates. Additionally, the studies illustrated in this article show that PANI electrochemical wrapping of SWCNT-based electrode led to substantial reduction in the electrode impedance. The two last findings suggested the potential of creating a composite material based on SWCNT/conductive polymers or especially SWCNT/PANI complexes as a promising neuro-electronic hybrid, enabling to control or improve neurite adhesion and outgrowth on CNT.

In this work, we report an electrochemical method for wrapping carbon nanotubes with the above mentioned conductive polymers and the characterization of their interaction potency. Based on the cytophilic properties of positively charged polymers and the intrinsic π-conjugation, we expect to improve the biocompatibility and conductivity of bare SWCNT. Improving the conductivity and thus reducing the electrode impedance, one should reduce the current threshold for neurons excitation and therefore reducing the risk of neuron damage. We have observed that the tightest wrapping of SWCNT occurs with PANI by the so-called surface attenuated infrared absorption (SAIRA) effect [31].

2. Experimental methods

2.1. Materials and processes

2.1.1. Materials

The SWCNTs used in this work were purchased from Sigma–Aldrich (Part No. 652512). The SWCNTs were synthesized by CVD (chemical vapor deposition) method and have a diameter of 1–2 nm and length of 0.5–2 μm. Aniline (ACS grade) was vacuum distilled before use. All of the reagents and solvents in this work are commercial products at analytical reagent (AR) grade, and triple distilled water (TDW) was used to make solutions.

The substrate used for FTIR measurements of the various pristine and hybrid SWCNTs is a gold layer with a thickness of 200 nm on 1.1 mm borosilicate glass with an about 15 nm Cr as an adhesion layer. The gold substrates were hydrogen flame annealed to achieve highly smooth surfaces with Au (111) terraces larger than $100 \times 100\ nm^2$.

2.1.2. SWCNT purification

Raw SWCNTs (1 g) were dispersed in about 130 mL of 2.6 M nitric acid solution and the mixture was refluxed for 48 h, then the supernatant was decanted off and the residue (SWCNTs) washed with TDW. The SWCNTs solution was then neutralized till pH 7 and sonicated under degassing mode at room temperature until the SWCNTs were dispersed. Finally, the purified SWCNTs were collected by vacuum filtration through polycarbonate membrane filter with porosity of 1 μm to remove the small pieces of SWCNTs eventually generated during the sonication. At last, the residue was dried in vacuum oven at 160 °C for 24 h.

2.1.3. Determination CNTs degree of functionalization

The purified product, oxidized SWCNT (assigned as SWCNT below), was dissolved in NaOH solution at pH 14 by sonication. Following dissolution in the base, the tubes were centrifuged at 10,000 rpm. The solid was then washed by 3.8 ml portions of TDW until the amount of sodium in the supernatant was undetected by atomic absorption. Following this washing, the solid was dried in vacuum oven at 80 °C for 16 h and weighed. Four milligram of dry solid were immersed in 3.8 ml of HNO_3 solution at pH 1, and sonicated for 30 min. The solution was then filtered and the atomic absorption was performed to measure the amount of sodium.

2.1.4. Gold slides cleaning

Prior to modifying the gold surface, the gold layer on the borosilicate substrate was cleaned according to the following procedure: firstly it was rinsed with 2-propanol and dried under flowing nitrogen, then cleaned by UV ozone cleaner (UVOCS) and finally immersed in ethanol for 20 min and dried again under nitrogen flow. The gold surface was coated with SWCNT and the conducting polymers PANI, PCz and melanin according to the same protocol as ITO (see "Preparation of Samples").

2.1.5. ITO slides cleaning

Untreated ITO (Indium Tin Oxide) coated glass slides (Delta Technologies) were sonicated for 30 min in *soapy water* (0.5 vol.%) at 60 °C, and then washed three times with TDW. After washing, the slides were sonicated in ammonium hydroxide solution ($H_2O/H_2O_2/NH_3$ 5:1:1 v/v/v) for 30 min, then washed again three times with TDW. Finally the ITO was rinsed with acetone and dried for 10 min at 130 °C. To prevent etching of the ITO, treatment with piranha solution was omitted. ITO glasses were used immediately following cleaning.

2.1.6. Preparation of samples

Sample A: ITO coated with oxidized SWCNT – 2.6 mg of purified and oxidized SWCNT were dissolved in 2 mL DMF (N,N-dimethyl formamide) by sonication for 5 min (solution I), then 0.1 mL of solution I were diluted to 5 mL with DMF (solution II). 0.1 mL of solution II was deposited dropwise by micropipette on an ITO slide. Finally the solvent was dried by N_2 flow and the residues were evaporated in vacuum oven.

Sample B: *Coating SWCNT with PCz* – Electrochemical polymerization has been performed by cyclic voltammetry (CV) on ITO coated by SWCNT (prepared as specified above for sample A) serving as the working electrode, Pt wire as counter electrode and Ag/AgCl as reference electrode, the voltage applied in the range of 0–1.3 V and 10 scans were carried at a scan rate of 50 mV/s. Electrolyte solution is composed of 0.1 M sodium perchlorate in Acetonitrile saturated with carbazole.

Sample C: *Coating SWCNT with PANI* – Electrochemical polymerization has been performed by CV on ITO coated by SWCNT working electrode (prepared as specified above for sample A), a Pt counter electrode and an Ag/AgCl reference electrode. The applied voltage was in the range −0.5 to 1.2 V, and 10 scans were carried out at a scan rate of 50 mV/s. The electrolyte was 0.1 M aniline in TDW solution at pH 3.5.

Sample D: *Coating SWCNT with melanin* – The working, counter and reference electrodes were ITO coated with SWCNT, a Pt wire and Ag/AgCl, respectively. The voltage applied was in the range of −0.5 to 1.0 V and 10 scans at a scan rate of 2 mV/s. The electrolyte was 4 mM dopamine in 0.1 M phosphate buffer solution and 0.5 M potassium chloride at the solution of pH 7. In all solutions, oxygen was removed by purging by high-purity nitrogen gas.

All substrates were washed three times in TDW dried with 2-propanol and kept sealed under N_2 prior to their use.

2.2. Characterization

2.2.1. Impedance measurements

The AC impedance measurements with alternating voltage amplitude of 5 mV between 20 and 250 MHz were conducted by using AUTOLAB PGSTAT12 (Eco Chemie B.V.). Measurements for all samples were performed in aqueous solution of 5.0 mM ferric cyanate ($K_3Fe(CN)_6$), 5.0 mM ferrous cyanate ($K_4Fe(CN)_6$), and 100 mM potassium chloride at a constant potential of 0.17 V, and with a Pt counter electrode and an Ag/AgCl reference electrode.

2.2.2. Infrared spectroscopy

Infrared spectra were taken by two FTIR instruments (Bruker Tensor 27 in the infrared/near infrared and Bruker IFS 66v in the far-infrared/infrared). Samples were deposited on glass/gold electrodes and were measured in reflectance mode. Absorbance spectra reported here are results of converting the obtained transmission to optical density $-\log T$. In the infrared/near infrared range we also employed a microscope in reflectance mode and collected spectra of various parts of the sample, to observe the homogeneity of the coatings. Identical spectra resulted, both in the infrared and near-infrared wavelength range, and the difference was caused by layer thickness which varied throughout the samples.

2.2.3. UV–VIS–NIR spectroscopy

Absorption spectra were recorded on a Shimadzu UV-310PC scanning spectrophotometer. The UV spectra was recorded on clean ITO, ITO coated with each of the polymers, SWCNT coated ITO and ITO coated first with SWCNT then with each polymer. The UV spectrum of each pure polymer was received by subtraction of the ITO spectrum from that of ITO coated with PANI, PCz and melanin; the UV spectra of SWCNT received by subtraction of the ITO spectra from the SWCNT coated ITO spectra. The spectra of each polymer on SWCNT were received by subtraction of the ITO/SWCNT spectra from that of ITO/SWCNT/conductive polymer polymerized on the same slide.

2.2.4. Electron microscopy and AFM (Atomic Force Microscopy)

High Resolution Scanning Electron Microscope (HRSEM) images were carried out on a FEI Sirion system for the hybrids ITO/SWCNT/PANI deposited on glass–ITO substrates. The AFM images were acquired in ambient using a nanotech Electronica S.L System in dynamic mode, soft, non-conductive, rectangular, commercial SiN cantilevers (OMCL-RC800PSA, Olimpus Optical Co. LTD) with quality factor (Q) $\sim$ 100, spring constant of 0.4–0.8Nm^{-1}, resonance frequency of 75–80 kHz and tip radius of 15 nm were used.

3. Results and discussion

3.1. Purified SWCNT

As a first step, to fully exploit the properties of SWCNTs, effective purification was needed to remove the amorphous carbon and catalyst residues. Various previously reported purification procedures were tested and an optimized method has been devised (see previous section for details) [32–34]. Characterization of the purified oxidized SWCNT was conducted by EDX, TEM, SEM, TGA (Thermo-gravimetric analysis), FTIR and Raman spectroscopy (see Supporting Information Figs. S1–6, respectively) and the following results were received. The purity and ash content in weight% derived from TGA is 95.76 and 1.24 respectively. The TGA thermogram, see Fig. S4, shows quantitatively that the weight percent of metals decrease from 9.61% to 1.24% by the purification protocol whereas the EDX spectrum, see Fig. S1, shows that most of metals were removed by this purification protocol, except Ga and oxygen which are of oxides origin. FTIR spectra show that the difference between the raw SWCNT and the purified one is the appearance of peaks in the latter at 1712 and 1722 cm^{-1}. These peaks correspond to the carbonyl groups of carboxylic acid attached to the open ends of the purified SWCNT. The degree of functionalization of SWCNT was determined by atomic absorption spectroscopy. This determination is based on the exchange of the acidic protons using NaOH, followed by the dilution of the conjugates with HNO_3 solution at pH 1. The acidification releases Na^+ ions that are quantified by atomic absorption. Based on calibration curve we found that 32 ppm w/w of carboxylate groups were present on functionalized SWCNT, corresponding to 1 carboxylic acid per 120,000 carbon atoms.

Due to purification, the D/G ratio determined by Raman spectroscopy grew from 0.37 ± 0.08 to 0.46 ± 0.05, respectively. Raman spectra were recorded using Ar^+ laser at 514 nm.

3.2. Voltammetry of polymerization

ITO slides were coated with SWCNT, then the samples were assembled with the conductive polymers PANI, PCz and mel-

anin by electrochemical polymerization followed by electrochemical, morphological and spectroscopic characterizations.

The electrochemical polymerization was performed by CV and the voltammograms for each electropolymerization are shown in Fig. 1. Cyclic voltammetry for electrochemical polymerization of aniline on the working electrode ITO coated with SWCNT (Fig. 1A) shows 10 oxidative cycles. As an example, in each cycle we can see the characteristic anodic 0.04–0.70 V (oxidation) and cathodic −0.2 to 0.6 V (reduction) peaks for PANI formation. The area and current of these peaks grow gradually during the cycles. Peak area growth following each cycle shows a monotonic accumulation of PANI on SWCNT. The broad oxidation and reduction peaks come from generation of oligomers at the first steps of the polymerization which grow during the cycles to yield the polymer. One other irreversible oxidation peak is the aniline monomer peak which appears around 0.88 V and decays during the oxidative cycles due to consumption of monomer during polymerization. In the same manner, the CV for carbazole electropolymerization on ITO coated with SWCNT (Fig. 1B) shows the characteristic cathodic and anodic peaks at about 0.78–0.90 and 0.95–1.00 V, respectively. The more complex CV is observed for electropolymerization of 4 mM dopamine in a pH 7.0 phosphate buffer solution on ITO coated CNT electrode (Fig. 1C), where the first scan shows two anodic peaks at 0.38 and 0.58 V, marked as A and B, respectively. The area and current of these peaks decay gradually during the oxidative cycles due to consumption of monomer and the intermediates generated during polymerization. Upon reversal of the potential scan from 1.10 V two cathodic peaks (C and D) were observed at 0.25 and −0.45 V respectively. Moreover in the second cycle a new anodic peak (E) appears at about −0.36 V. The polymerization steps of dopamine to melanin can be explained by generating the species illustrated Fig. 2, peaks A and B correspond to the oxidation of dopamine (**1**) to the open-chain dopaminequinone (**2**) and peak C corresponds to the reduction of dopaminequinone to dopamine which are in equilibrium. From the cyclic voltammogram it is evident that the redox of dopamine is an irreversible process. Peaks D and E are attributed to the redox of the cyclized product dopaminechrome (**4**) [35] – leucodopaminechrome (**3**) couple [36]. The accepted polymerization mechanism in aqueous solution at neutral pH involves the dipolar ion (**6**) in acid base equilibrium [37] which can be polymerized through the alkoxide or indole amine groups to give the melanin polymer. Furthermore it is important to note that it was clearly observed that the initially colorless solution generated a brown film which converted to black on the surface of the electrode during voltammetry. The CV of melanin on SWCNT sample measured in buffer solution and the resulting voltammogram illustrated in Fig. 1C show that the anodic and cathodic peaks of melanin on SWCNT are at 0.7 and 0.9 V respectively.

Fig. 3 shows the HRSEM images of an SWCNT slide uncoated (Fig. 3A), and coated by PANI as an example. The images show a uniform coating, obtained by coating at various conditions. In 0.1 M electrolyte concentration (Fig. 3B) received a thin layer which cover the SWCNT but do not bury them, as in the higher electrolyte concentration (Fig. 3C). These observations guide us to optimize polymerization conditions, in order to obtain a uniform coating, while maintaining SWCNT 3D structure.

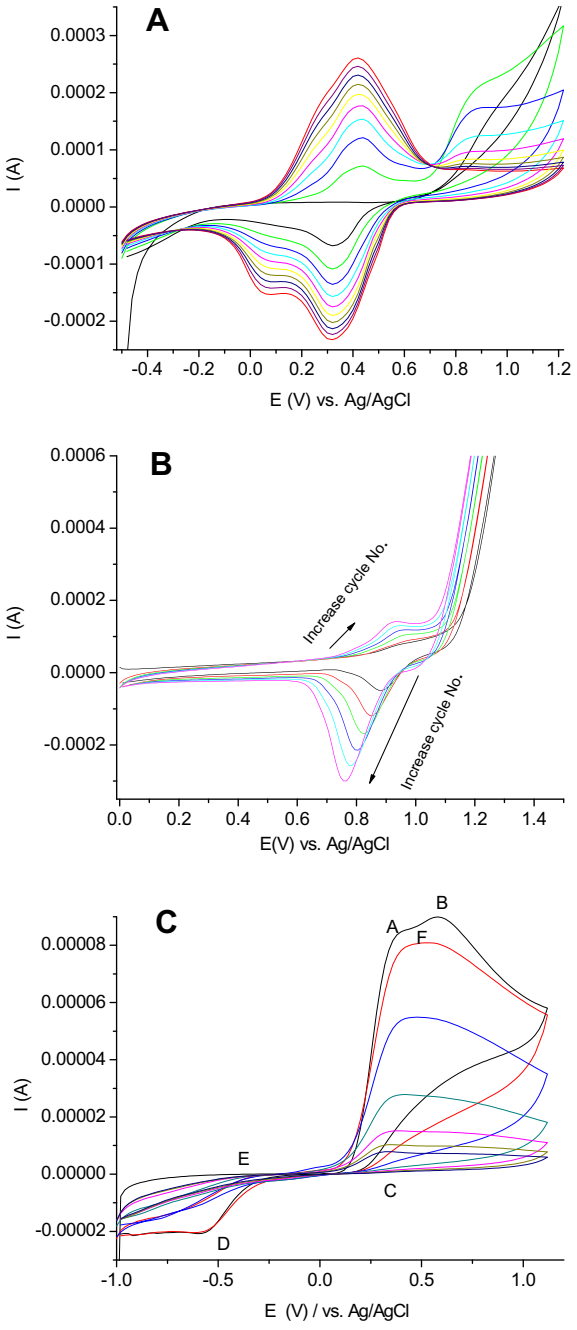

Fig. 1 – Cyclic voltammetry (CV) of electrochemical polymerization of carbazole (1A) aniline (1B) and Dopamine (1C) on ITO coated SWCNT. The voltammograms in A were performed in a voltage range of 0.0–1.3 V, at scan rate of 50 mV/s and the electrolyte is: 0.01 M carbazole in 0.1 M Sodium Perchlorate ($NaClO_4$) in Acetonitrile. The voltammograms in B recorded in a voltage range of −0.5 to 1.2 V, at scan rate of 50 mV/s and 0.1 M aniline solution in TDW with pH corrected to 3.5 used as electrolyte and C were performed in a voltage range of −1.0 to 1.1 V, at scan rate of 2 mV/s and the electrolyte is: 4 mM Dopamine in PBS (phosphate buffer saline) solution at pH 7.

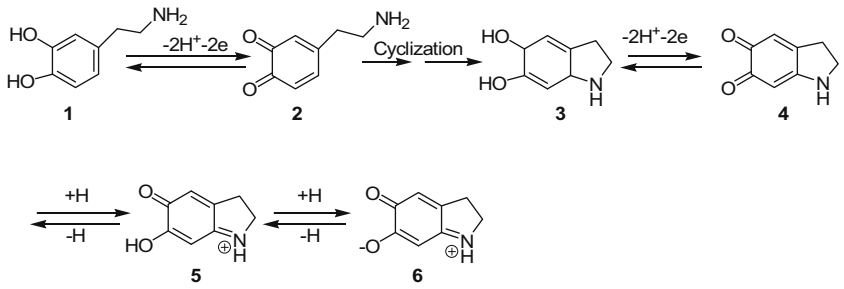

Fig. 2 – IIntermediate species generated along the polymerization steps of dopamine to melanin. (1) Dopamine, (2) dopaminequinone, (3) leucodopaminecgrome, (4) dopaminechrome, (5) *p*-quinoemine and (6) *p*-quinoemine dipolar ion.

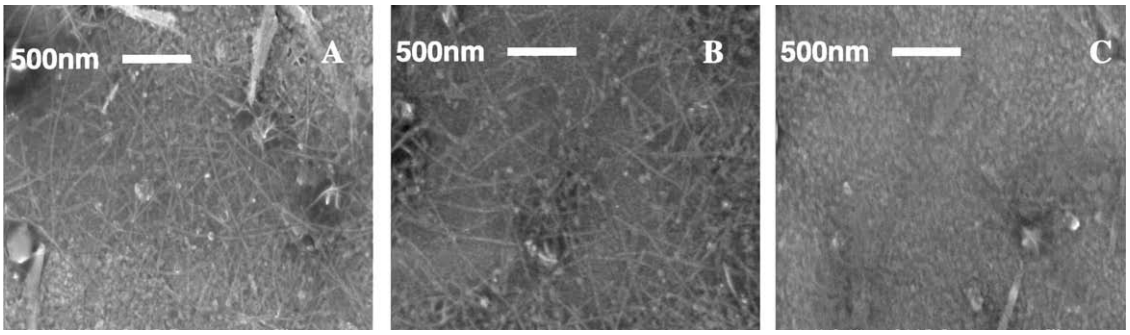

Fig. 3 – SEM images of SWCNT on ITO before and after electropolymerization. with PANI: SWCNT on ITO before coating (A), SWCNT on ITO coated with PANI by using 0.1 M aniline solution as electrolyte, 10 scans at rate of 50 mV/s (B). SWCNT on ITO coated with PANI in the following conditions: Two scans at rate of 50 mV/s and 0.5 M aniline solution as electrolyte (C).

Fig. S7 shows an AFM image (Figs. S7–1) of the gold surface used for roughness determination, RMS roughness = 1.36 nm. Terrace of SWCNT generated on the gold surface (see Section 2.1.6.) and a terrace of each conducting polymer generated on the SWCNT coated gold surface by electrochemical polymerization as described above. The height of the different terraces detected by profilometry and the derived thickness of SWCNT (3A), PCz (3B), PANI (3C) and melanin (3D) are: 107 ± 23 nm, 280 ± 18 nm, 355 ± 20 nm and 302 ± 15 nm (n = 10) respectively.

Roughnesses of the films were also determined by AFM and are 30, 16, 19 and 12 nm respectively. From this results we can say that the roughness of the gold surface does not need to be taken in consideration when we compare it to the conductive polymers film thickness, thus substrate annealing is not crucial for this study.

3.3. *AC impedance spectra*

The effect of the electropolymerized conductive polymers PANI, PCz and melanin coating on the ITO/SWCNT-based electrode impedance is reflected in the data of Fig. 5. Comparison of the impedance of ITO/conductive polymer and ITO/SWCNT-based electrodes to ITO/SWCNT/conductive polymer based electrodes demonstrates a clear drop in impedance when SWCNT is coated with conductive polymers. These results mean that the addition of a conductive polymer improves the electron transfer to the ionic solution by reducing the impedance of the electrode. Such improved conductance is manifested as a lower resistance to electron transfer (R_{et}), thus the electron transfer from the electrolyte to the ITO/SWCNT/conductive polymer surface is easier than to the ITO/SWCNT surface (Table 1). The R_{et} value of 2210 Ω for SWCNT decreases to 344 Ω for PCz, 142 Ω for PANI and to 1293 Ω for Melanin coated SWCNT, respectively Fig. 4.

The degree of reduced impedance depends on the morphology-conductivity of the conductive polymer: assuming a similar increase in surface area the more conductive ones give lower impedance. These results show that PANI, which has the best electrical conductivity (~1 S/cm) [38] among the conducting polymers investigated in this study, gives the most pronounced decrease in the hybrid electrode's impedance, followed by PCz (with a conductivity of ~1 mS/cm) [39] and finally melanin which has the lowest conductivity (~1 μS/cm) [40]. SWCNT layer thickness effect on the impedance measured (see also Fig. S8) show that the R_{et} increase as the layer thickness increase this result mean that the decrease in R_{et} of the hybrid SWCNT/conducting polymer does not originate from layer thickness increase.

Table 1 – Solution resistance (R_s), electron transfer resistance (R_{et}) and capacity (C) of the various modified ITO electrodes.

Electrode name	R_s (Ω)	R_{et} (Ω)	C_{dl} (F/cm^2)
SWCNT	66	2210	5.37×10^{-7}
PANI	65	1042	3.99×10^{-12}
SWCNT–PANI	64	142	9.57×10^{-8}
Melanin	65	15,440	4.69×10^{-8}
SWCNT–Melanin	66	1293	2.74×10^{-8}
PCz	65	1524	2.53×10^{-10}
SWCNT–PCz	66	344	1.23×10^{-5}

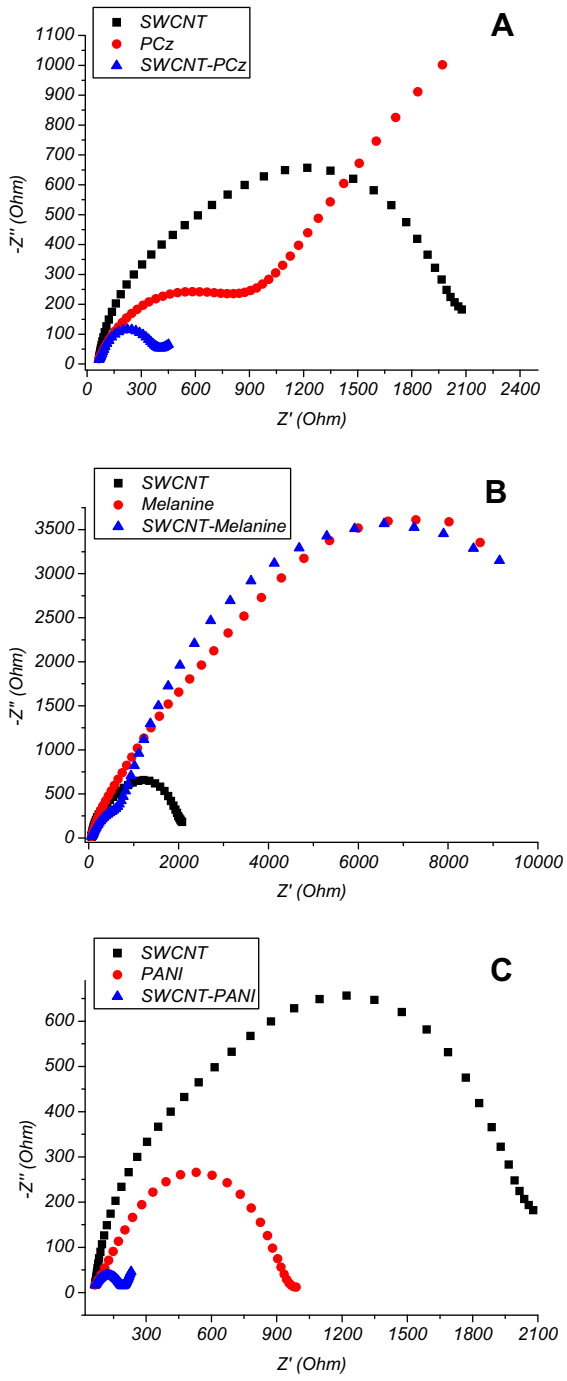

Fig. 4 – AC impedance spectroscopy, Niquest plot (Z″ versus Z'), of the conductive polymers PCz pure, PCz–SWCNT and SWCNT on ITO (A), Melanin pure, SWCNT and Melanin–SWCNT on ITO (B), and of PANI pure, SWCNT and PANI–SWCNT on ITO (C), the impedance measured in a water solution of 5.0 mM $K_3Fe(CN)_6$, 5.0 mM $K_4Fe(CN)_6$ and 100 mM KCl at constant potential of 0.17 V.

3.4. *UV–VIS–NIR spectra*

Fig. 5B–D shows the UV–VIS–NIR spectra of each pure polymer compared to the spectrum of each polymer in the hybrids with SWCNT. For comparison, the spectrum of SWCNT is also given in Fig. 5A. The SWCNT has two characteristic absorption bands with maxima at around 1100 and 600 nm which are the S_{22} transition of semiconducting tubes and the M_{11} transition of metallic tubes respectively [41]. Different sections or slit width in the same coated slide show a small variability in the absorbance spectra which demonstrate homogenous SWCNT dispersion on the slide (see S.I. Fig. S7). Moreover we illustrate in Fig. 5 the observed shifts on the same slide which its absorbance spectra measured after each treatment (Bare ITO, ITO + CNT and ITO + CNT + -PANI) as described in Section 2.2.3.

The PANI spectrum is dominated by two broad absorption bands: the first band at 550 nm is assigned to the benzoid–quinoid transition in the emeraldine form; the second absorption peak at about 1100 nm is due to the transition from the valence to the polaronic band [42]. The spectrum of PCz has features at about 370 and 620 nm due to the two different dicarbazyl cation radicals determining the structure during electropolymerization [43]. Melanin shows a spectrum of broad absorption bands at 1200, and 541 nm. We can not evaluate the exact structure of melanin which we received because of the insolubility of the powder in various polar and non-polar solvents.

The spectra show that PANI, PCz and melanin on SWCNT shift their absorption bands to longer wavelengths in comparison to the pristine materials on ITO. This implies that the interaction between each of these conducting polymers and SWCNTs leads to a π-conjugated system as evident by the red shift of the polaron bands. The shift of PCz and PANI seem to be larger than that of melanin, indicating a stronger interaction with the SWCNTs' π-orbitals, *vide infra*.

3.5. *Infrared and Raman spectra*

Infrared and near-infrared spectra of conducting polymer wrapped nanotubes, compared with those of the constituents for all materials, are shown in Fig. 6. The substrate in all of these measurements is a gold surface and it is used as a reference. In the left panel, we concentrate on the electronic excitations of which the most pronounced are those of the S_{11} electronic transition of the semiconducting nanotubes around 5300 cm^{-1}. This feature appears in all three hybrid materials Fig. 6.

In the right panel, we show the part of the spectrum containing molecular vibrations of the polymer coating materials (in this region, the SWCNT spectrum is featureless). Compared to the pure polymers, we observe some distinct changes. For the carbazole hybrid, although the vibrational mode of the BF_4^- ion at 1080 cm^{-1} indicates the presence of the polymer, the carbazole modes [8,44] are much weaker. This effect is even stronger for PANI-wrapped tubes: the PANI vibrations are considerably weaker than expected from the infrared spectrum of the pure material (most probably the emeraldine base form [45] some vibrations completely disappear. The latter, disappearing bands (at 1150, 1500 and 1590 cm^{-1}) have been assigned as benzenoid or quinoid modes, all in-plane polarized [45,46]. In the melanin hybrid the spectra are much more similar before and after coating.

This effect, surprising at first sight, was previously seen on poly(*p*-phenyleneethynylene) adsorbed on nanotube surfaces by Setyowati et al.[31] and was termed SAIRA (Surface Atten-

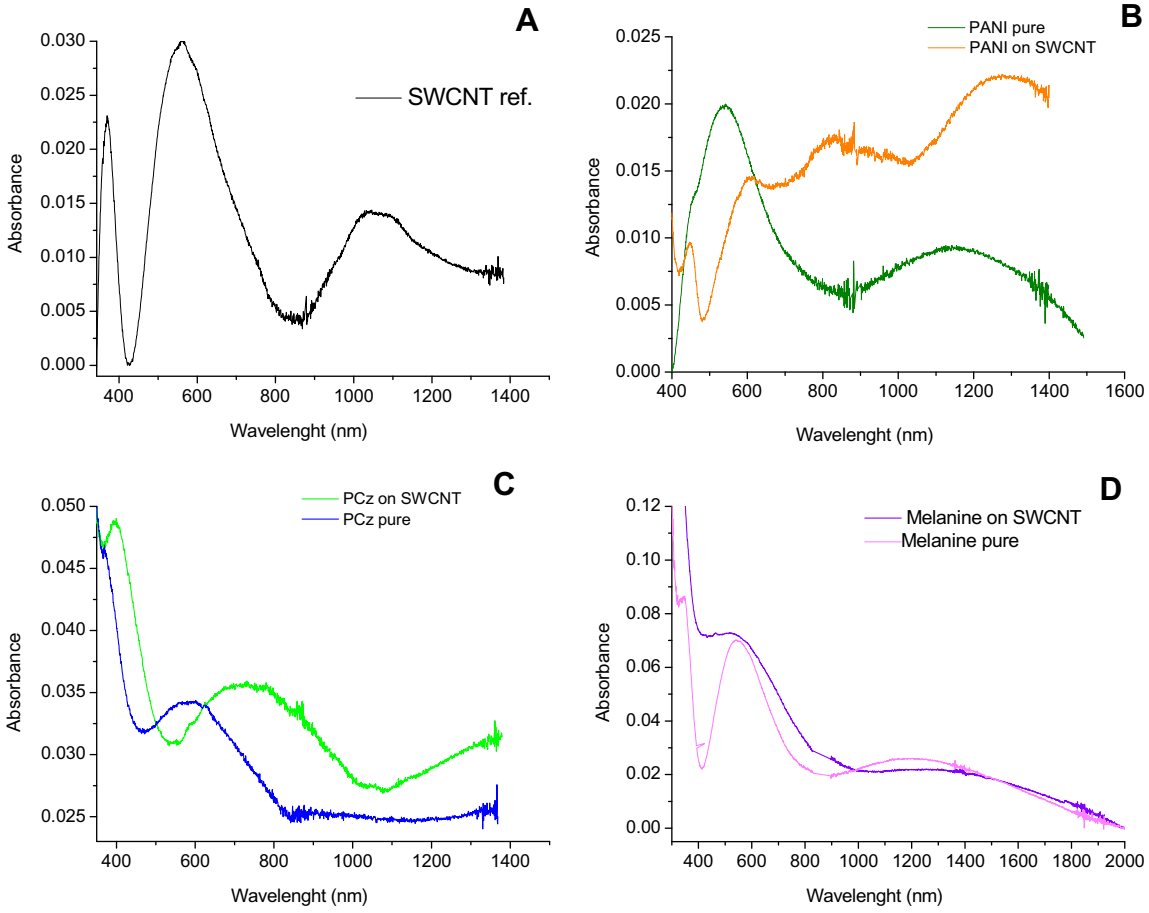

Fig. 5 – UV–VIS–NIR differential spectra of SWCNT (4A) and of the conductive polymers PANI (4B), PCz (4C) and Melanin (4D), coated on clean ITO and on ITO coated SWCNT; see Experimental Section for details.

uated Infrared Absorption). The effect originates in the image dipoles on the polarizable surface of the nanotube, which cause a vibrational motion of charges opposite to that of the molecule adsorbed on the tube. As a result, the net dipole change during the vibration weakens and can become close to zero, resulting in intensity loss of the corresponding vibrational mode. A prerequisite for the image charge to form is that the vibrating dipole is parallel to the surface [47] which is fulfilled by the benzene rings of both PANI and carbazole if we assume that the principal interaction between the polymer and the SWCNT is π–π stacking.

For the image charge to be formed, an intimate contact between the nanotube and the adsorbed molecule is necessary. Setyowati et al. [31] characterized various nanotube surfaces according to the SAIRA effect with one macromolecule; in the present study, we hold the nanotube constant and attempt a classification of the wrapping molecules based on the strength of the interaction with the nanotube surface. The degree of SAIRA depends on the distance between the adsorbed molecules and the nanotube surface, as well as the quality of the nanotube surface and the strength of the π–π interaction between the nanotube and the adsorbent. Since the nanotubes used in all three cases were identical, the attenuation should reflect the strength of the π–π interaction. Based on these considerations, the interaction with the SWCNT proved to be strongest for PANI, followed by PCz and then melanin.

Raman spectra of PANI–SWCNT hybrids present additional evidence for the strong interaction. Contrary to the other two materials, where the Raman spectra are dominated by nanotube features, in this case the intense PANI Raman bands at 1181, 1383 and 1513 cm^{-1} are clearly discernible (Fig. 7). A possible explanation for this phenomenon is an enhancement of Raman intensity by the image charge, similar to the SERS mechanism.

Thus we find a common explanation for the changes in both types of vibrational spectra, and attribute it to the strong π–π interaction between the aromatic rings and the surface of the nanotubes, especially in the case of polyaniline. Our results are similar to those of Baibarac et al. [48] at low PANI coverage; we did not increase the polymer content further because we wanted to optimize and not maximize coverage of our nanotubes. The authors of Ref. [48] propose covalent sidewall functionalization as the type of bonding in PANI–SWCNT; in view of the above spectral changes, we conclude that the typical structure of nanotube-polymer hybrids is rather non-covalent wrapping, as is the case with other polymers [49].

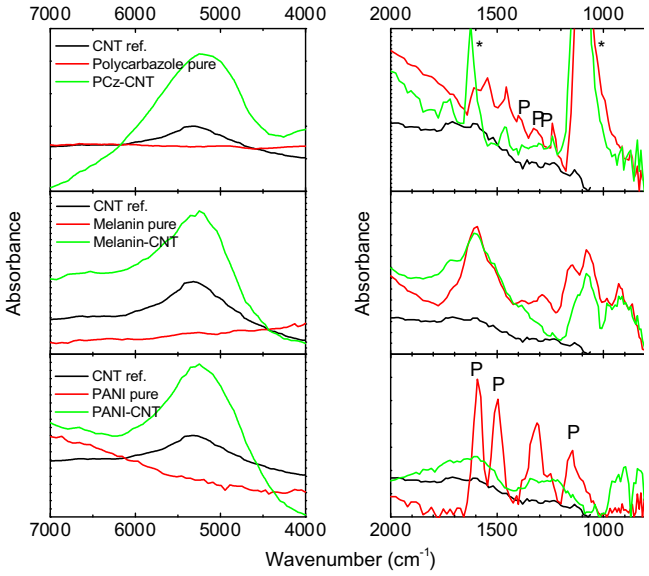

Fig. 6 – *Left panel*: NIR spectra of conducting polymers wrapped carbon nanotubes and their constituents. The typical CNT transition around 5300 cm^{-1} is visible in the hybrid structures as well. *Right panel*: IR spectra of the hybrid materials and their constituents in the range of molecular vibrations. In the carbazole and PANI–CNT hybrid compounds, some of PANI vibrations show up with decreased intensity, due to the SAIRA (surface attenuated infrared absorption) effect. These vibrations are denoted by P. Asterisks indicate extrinsic features (counter ion, and atmospheric absorption).

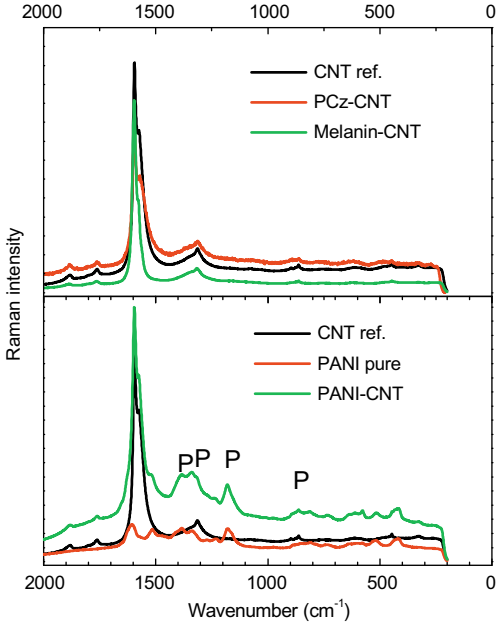

Fig. 7 – *Bottom panel*: Raman spectra of PANI, SWCNT and the hybrid material taken with 785 nm laser excitation. The hybrid material shows the Raman peaks of both constituents (polymer peaks are denoted by P). *Top panel*: Raman spectra of SWCNT, PCz–SWCNT and Melanin–SWCNT. The latter two spectra show no difference from pristine SWCNT.

Acknowledgment

This research was supported by the European Commission through the research project NEURONANO (NMP4-CT-2006-031847).

Appendix A. Supplementary data

Supporting information includes FTIR, HRSEM, EDX, and Raman spectra of our purified SWCNT. Supplementary data associated with this article can be found, in the online version, at doi:10.1016/j.carbon.2010.04.005.

REFERENCES

[1] Xiao Q, Zhou X. The study of multiwalled carbon nanotube deposited with conducting polymer for supercapacitor. Electrochemica Acta 2003;48:575–80.
[2] Frackowiak E, Beguin F. Carbon materials for the electrochemical storage of energy in capacitors. Carbon 2001;39:937–50.
[3] Roth S, Burghard M, Leising G. Molecular materials for electronic and optical applications. Curr Opin Solid State Mater Sci 1998;3:209–15.
[4] Ferrer-Anglada N, Kaempgen M, Roth S. Transparent and flexible carbon nanotube/polypyrrole and carbon nanotube/polyaniline pH sensors. Phys Stat Sol 2006;243:3519–23.
[5] Smart SK, Cassady AI, Lu GQ, Martin DJ. The biocompatibility of carbon nanotubes. Carbon 2006;44:1034–47.
[6] Qiao Y, Li CM, Bao S-J, Bao Q-L. Carbon nanotube/polyaniline composite as anode material for microbial fuel cells. J of Power Sources 2007;170:79–84.
[7] Kim JY, Kim KH, Kim KB. Fabrication and electrochemical properties of carbon nanotube/polypyrrole composite film electrodes with controlled pore size. J of Power Sources 2008;176:396–402.
[8] Baibarac M, Lira-Cantu M, Oro-Sole J, Casan-Pastor N, Gomez-Romero P. Electrochemically functionalized carbon nanotubes and their application to rechargeable lithium batteries. Small 2006;2:1075–82.
[9] Lota K, Khomenko V, Frackowiak E. Capacitance properties of poly(3, 4-ethylenedioxythiophene)/carbon nanotubes composites. J Phys Chem Solids 2004;65:295–301.
[10] Biju P, Jining X, Anupama C, Jose A, Vijav KV. A novel nanocomposite from multiwalled carbon nanotubes functionalized with a conducting polymer. Smart Mater Struct 2004;13:295–8.
[11] Meredith P, Riesz J. Techniques for delivery and monitoring of TOOKAD (WFT09)-mediated photodynamic therapy of the prostate clinical experience and practialities. Photochem Photobiol 2004;79:211–22.
[12] Hamilton AJ, Gomez BL. Melanins in fungal pathogens. J Med Microbiol 2002;51:189–91.
[13] Tian S, Garcia-Rivera J, Yan B, Casadevall A, Stark RE. Unlocking the molecular structure of fungal melanin using C-13 biosynthetic labeling and solid state NMR. Biochemistry 2003;42:8105–9.
[14] Macit H, Sen SM, Sacak M. Electrochemical synthesis and characterization of polycarbazole. J Appl Polym Sci 2005;96:894–8.
[15] Saxena V, Shirodkar V, Parakash R. Copper (II) ion-selective microelectrochemical transistor. J Solid State Electrochem 2000;4:234–6.

[16] Abe Y, Bernede JC, Ugalde L, Tregouet Y, Del Valle MA. Electrochemical deposition of polycarbazole thin films onto tin oxide coated glass: physicochemical and optoelectronic characterizations. J Appl Polym Sci 2007;106:1568–75.
[17] Pandey PC, Prakash R, Singh G, Tiwari I, Tripathi VS. Studies on polycarbazole-modified electrode and its applications in the development of solid-state potassium and copper(II) ion sensors. J Appl Polym Sci 2000;75(14):1749–59.
[18] Kobayashi N, Kijima M. Blue electroluminecent properties of poly(N-arylcarbazole-2, 7-ylene) homopolymers. Appl Phys Lett 2007;91:081113–5.
[19] Lim JY, Ko HC, Lee H. Single- and dual- type electrochromic devices based on polycarbazole derivative bearing pendent viologen. Synth Met 2006;156:695–8.
[20] Blouin N, Michaud A, Gendron D, Wakim S, Blair E, Plesu RN, et al. Toward a rational design of poly(2,7-carbazole) derivatives for solar cells. J Am Chem Soc 2008;130:732–42.
[21] Parpura V. Carbon nanotubes on the brain. Nature Nanotech 2008;3:384–5.
[22] Keefer EW, Botterman BR, Romero MI, Rossi AF, Gross GW. Carbon nanotube coating improves neuronal recordings. Nature Nanotech 2008;3:434–9.
[23] Cohen A, Shappir J, Yitzchaik S, Spira ME. Experimental and theoretical analysis of neuron transistor hybrid electrical coupling: The relationships between the electro-anatomy of cultured Aplysia neurons and the recorded field potentials. Biosens Bioelectron 2006;22:656–63.
[24] Mattson MP, Haddon RC, Rao AM. Molecular fanctionalization of carbon nanotubes and use as substrates for neuronal growth. J Mol Neurosci 2000;14:175–82.
[25] Hu H, Montana Y, Ni V, Haddon RC, Parpura V. Chemically functionalized carbon nanotubes as substrates for neuronal growth. Nano Lett 2004;4:507–11.
[26] Lovat V, Pantarotto D, Cacciari B, Grandolfo M, Righi M, Spalluto G, et al. Carbon nanotube substrates boost neuronal electrical signaling. Nano Lett 2005;5:1107–10.
[27] Mazzatenta A, Giugliano M, Campidelli S, Gambazzi L, Businaro L, Markram H, et al. Interfacing neurons with carbon nanotubes: elctrical signal transfer and synaptic stimulation in cultured brain circuits. J Neurosci 2007;27:6931–6.
[28] Gabay T, Ben David M, Kalifa I, Sorkin R, Abrams ZR, Ben–Jacob E, et al. Electro-chemical and biological properties of caron nanotube based multi-electrode arrays. Nanotechnology 2007;18:035201.
[29] Sfez R, Peor N, Cohen S, Cohen H, Yitzchaik S. In-situ SFM Study of 2D-polyaniline surface confined enzymatic polymerization. J Mater Chem 2006;16:4044–50.
[30] Oren R, Sfez R, Korbakov N, Shabtai K, Cohen A, Erez H, et al. Electrically conductive 2D-PAN-containing surfaces as a culturing substrate for neurons. J Biomater Sci Polymer Edition 2004;15:1355–74.
[31] Setyowati K, Piao MJ, Chen J, Liu H. Carbon nanotube surface attenuated infrared absorption. Appl Phys Lett 2008;92:043105/1–3.
[32] Liu J, Rinzler AG, Dai H, Hafner JH, Bradley RK, Boul PJ, et al. Fullerene pipes. Science 1998;280:1253–6.
[33] Montoro LA, Luengo CA, Rosden JM, Cazzanelli E, Mariotto G. Study of oxygen influence in the production of single wall carbon nanotubes obtained by arc method using Ni and Y catalyst. Diamond Relat Mater 2003;12:846–50.
[34] Duesberg S, Muster J, Byrne HJ, Roth S, Burghard M. Towards processing of carbon nanotubes for technical applications. Appl Phys A: Mater Sci Process 1999;69:269–74.
[35] Shanxin X, Oi W, Yinghong C. Study on electrical conductivity of single polyaniline microtube. Mater Lett 2007;61:2965–8.
[36] Macit H, Sen S, Sacak M. Electrochemical synthesis and characterization of polycarbazole. J of Applied Polymer Science 2005;96:894–8.
[37] Subianto S, Will G, Meredith P. Electrochemical synthsis of melanin free-standing films. Polymer 2005;46:11505–9.
[38] Morris MD. Resonance raman spectra of the aminochromes of some biochemically important catechol amines. Anal Chem 1975;47:2453–4.
[39] Hawley MD, Tatawawadi SV, Piekarski S, Adams RN. Electrochemical studies of the oxidation pathways of catechol amines. J Chem Soc 1967;89:447–50.
[40] Barreto WJ, Ponzoni S, Sassi P. A Raman and UV-VIS study of catecholamines oxidized with Mn (III). Spectrochim Acta Part A 1999;55:65–72.
[41] Lehman JH, Hurst KE, Roberson LK, Hamlin JD. Inverted spectra of single-wall carbon nanotube films. J Phys Chem C 2008;112:11776–83.
[42] Huang WS, DacDiarmid AG. Optical properties of polyaniline. Polymer 1993;34:1833–45.
[43] Kessel R, Schultze JW. Surface analytical and photoelectrochemical investigations of conducting polymers. Surf Interface Anal 1990;16:401–6.
[44] Macit H, Sen S, Saçak M. Electrochemical synthesis and characterization of polycarbazole. J Appl Polym Sci 2005;96:894–8.
[45] McCall RP, Ginder MJ, Roe MG, Asturias GE, Scherr EM, MacDiarmid AG, et al. Massive polarons in large-energy-gap polymers. Phys Rev B 1989;39:10174–8.
[46] Quillard S, Louarn G, Lefrant S, Macdiarmid AG. Vibrational analysis of polyaniline: a comparative study of leucoemeraldine, emeraldine and permigraniline bases. Phys Rev B 1994;50:12498–608.
[47] Pearce HA, Sheppard N. Possible importance of a “metal-surface selection rule” in the interpretation of the infrared spectra of molecules adsorbed on particulate metals: infrared spectra from ethylene chemisorbed on silica-supported metal catalysts. Surf Sci 1976;59:205–17.
[48] Baibarac M, Baltog I, Godon C, Lefrant S, Chauvet O. Covalent functionalization of single-walled carbon nanotubes by aniline electrochemical polymerization. Carbon 2004;42:3143–52.
[49] O’Connell MJ, Boul P, Ericson LM, Huffman C, Wang Y, Haroz E, et al. Reversible water-solubilization of single-walled carbon nanotubes by polymer wrapping. Chem Phys Lett 2001;342:265–71.